Transmission of Elastic Pulses in Metal Rods*

D. S. HUGHES, W. L. PONDROM, AND R. L. MIMS**
Department of Physics, University of Texas, Austin, Texas
(Received January 20, 1949)

Pulses are generated at one end of a cylindrical rod by a quartz crystal. A second crystal at the opposite end is used as a detector. The transmission time is studied as a function of rod length, diameter, and material. In general a single input pulse gives rise to several pulses at the detector. For the dimensions and rise times used, all of the arrivals are explicable in terms of transmission with either the dilatational or rotational velocity of the material or a combination of both. The rotational and dilatational velocities can be computed from these data and hence the elastic constants of the material.

INTRODUCTION

A QUICK accurate method of measuring the elastic constants of solids has been the objective of much research, and many special methods have been evolved which are applicable to special conditions. The authors desiring a method applicable to small cylindrical samples have investigated the transmission of sharp pulses through samples of this form. Under certain conditions, all of the elastic constants of an isotropic solid may be determined from the transmission of pulses from one end of the cylindrical sample to the opposite end. It is necessary that the material be capable of transmitting pulses of the requisite rise time, i.e., 0.2 to 0.6 μsec., but only longitudinal excitation and detection is necessary. Good results have been obtained with steel, brass, aluminum, and Lucite.

THEORY OF THE EXPERIMENTAL METHOD

A block diagram of the apparatus is shown in Fig. 1. The cylindrical rods are driven by an x cut quartz crystal pressed against one end, and a similar crystal used as a detector or "pick-up" is pressed against the opposite end. These crystals are $1\frac{1}{8}$ inch in diameter and have a fundamental frequency of 3.5 megacycles for free longitudinal vibration in the direction of thickness.

A model TS-100/AP oscilloscope[1] is used as the basic time standard. This instrument has a circular sweep of 12.368 μsec. per revolution which is generated continuously from an 80.86-kc crystal oscillator. A trigger circuit can be synchronized at any submultiple of this frequency lying between 300 and 1500/sec. This circuit generates pulses accurately synchronized with the circular sweep and having a rise time of 0.1 μsec., duration 0.6 μsec., and amplitude of +100 volts or −70 volts. These trigger pulses can be used to synchronize a Brooton model 300-pulse generator, which in turn excites the crystal. The pulses from this generator can be varied in amplitude[2] and duration but have a longer rise time than those from the trigger generator of the TS-100/AP oscilloscope.

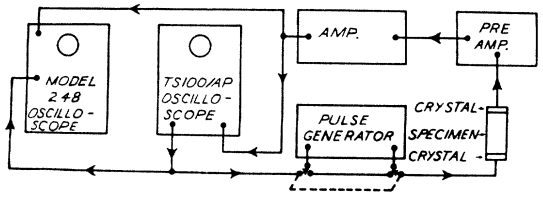

FIG. 1. Block diagram of apparatus.

The pick-up crystal is connected to a preamplifier and amplifier similar to that described by Jordan and Bell.[3] The output of this amplifier is connected to the vertical deflection plates of the Dumont model 248 oscilloscope and to the radial deflection electrode of the TS-100/AP oscilloscope. The fixed sweeps of the model 248 instrument are triggered from the pulse generator of the TS-100/AP instrument.

Using the 100-μsec. fixed sweep and 10-μsec. markers on the model 248 instrument the time of arrival of each pulse train can be read to 1 μsec. The character of the pulses is also easily checked with this presentation.

The TS-100/AP oscilloscope is used for the precise measurement of arrival times. The accuracy of reading this unit varies with the sharpness and amplitude of the arrival. For the better defined pulses different observers could repeat to about 0.03 μsec. The continuously running circular sweep causes no confusion of data from different revolutions because the instrument is provided with a variable delay intensity gate which allows the operator to select any desired revolution after the

* This work was supported by the ONR under Contract N6onr-266.
** Employed under research grant from Shell Oil Company.
[1] Radiation Laboratory Series Vol. 21, *Electronic Instruments* (McGraw-Hill Book Company, Inc., New York, 1948), pp. 626–634.
[2] A control has been added to this instrument which varies the screen grid potential of its output amplifier. This controls the pulse amplitude and has a slight influence on the rise time of the pulses.
[3] W. H. Jordan and P. R. Bell, "General purpose linear amplifier," Rev. Sci. Inst. 18, 703 (1947).

trigger and examine it separately. The trace is blanked out for all revolutions but the desired one.

A photographic record of the display obtained on the Model 248 oscilloscope is shown in Fig. 2. Traces *I* and *VIII* are simply records of the 10-μsec. markers. Trace *II* was taken with the two crystals in contact. The start of the pulse train is the small down-kick followed by a damped wave train (frequency about 1 megacycle). Trace *III* shows the arrivals with a steel rod 3.645 cm in diameter and 5.080 cm in length placed between the crystals. Traces *IV*, *V*, and *VI* are for rods of the same diameter, cut from the same stock, having lengths of 10.160 cm, 15.240 cm, 20.320 cm, and 25.400 cm, respectively. A clear sharp arrival at the points marked *A* with a character very similar to that of the directly coupled crystals in trace *II* is found for all rods. In addition there are clearly defined arrivals marked *B*, and on the longer rods arrivals marked *C*. For the longer rods many more such arrivals are visible on the TS-100/AP display. These arrive later than 100 μseconds after the trigger and are not recorded in this photograph. These arrivals can be brought into view on the model 248 display by triggering the 100-μsec. sweep from the delayed gate of the TS-100/AP oscilloscope. Table I shows the arrival times of all wave groups that could be clearly identified. On the basis of character these have been separated into two groups. Members of the first group show a character similar to the directly coupled crystal signal and their arrival times are denoted t_A, t_B, t_C, etc. in order of arrival. Members of the second group are indicated at *P* on traces *III* and *IV* and occur at much larger times on the longer rods. These are characterized by longer wave trains than those of the first group. These arrival times are given as t_P, t_Q, t_R, etc.

The arrival time, t_A, is evidently linear with rod length, and the corresponding velocity is 5886 meters/sec. This is much too high for a wave transmitted with the so-called bar-velocity, V_E, given by

$$V_E=(E/\rho)^{\frac{1}{2}}, \tag{1}$$

where E is Young's modulus and ρ is the density of the material. However, if we assume that this is a true dilatational wave, its velocity, V_D, should be given by

$$V_D=[(K+4\mu/3)/\rho]^{\frac{1}{2}}, \tag{2}$$

where K is the bulk modulus and μ is the shear modulus of the material. A computation of this velocity using handbook values of K and μ is in close agreement with the above experimental figure, and thus fits the hypothesis satisfactorily.

The arrivals at t_B, t_C, t_D, etc. are somewhat different. It is apparent from Table I, that the velocity of the waves corresponding to these arrivals is also

TABLE I. Arrival times of wave groups. $D=3.645$ cm, t in μsec

Rod No.	L cm	t_A	t_B	t_C	t_D	t_P	t_Q	t_R	t_S
20	2.54	4.27				13.05			
21	5.08	8.69				25.91	35.68		
22	10.16	17.23	27.15			51.90	61.51		
23	15.24	25.89	35.66			77.73	87.29		
24	20.32	34.72	44.34	53.86	63.32	103.58	113.10	122.88	
25	25.40	43.16	53.00	62.27	71.55	129.43	138.95	148.35	158.43

V_D, because the time intervals t_B-t_A, t_C-t_B, etc. are the same for all the various lengths of rods. These must then correspond to delayed wave trains, and, since the above intervals are equal for all of these rods, the delay is independent of the length of the rods.

Figure 3 is similar in all respects to Fig. 2 except that steel rods 2.540 cm in diameter were used. The corresponding data on arrivals are shown in Table II, and it is apparent that the arrivals at t_A correspond to the same velocity, V_D, as before. However, the intervals t_B-t_A, t_C-t_B, etc. from Table II are shorter than those of Table I but are constant for the rods considered in Table II. These intervals are shorter than those of Table I in the ratio 2.540/3.645 and lead to the conclusion that the delay is directly proportional to the diameter of the rods. It is thus apparent that these wave groups traveled during some part of the path in a direction oblique to the axis of the rod so as to traverse the diameter of the rod.

A rational explanation is obtainable from a consideration of the effect of the free surfaces bounding the rod. The driving crystal would be expected to generate a group of plane waves of dilatation at the driven boundary traveling very nearly parallel to the free cylindrical wall of the rod. It is well known that such waves cannot alone satisfy the free boundary condition, but must be accompanied by rotational waves.[4] In the present situation these rotational waves must travel very nearly at an angle θ relative to the normal of the boundary where θ is given by

$$\sin\theta=V_R/V_D, \tag{3}$$

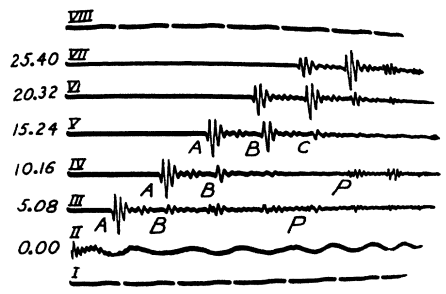

FIG. 2. Pulses through cold rolled steel rods 3.645 cm in diameter.

[4] *Handbuch der Physik*, Band VI (Verlag. Julius Springer, Berlin, 1928), pp. 323–324.

TABLE II. Arrival times of wave groups. $D=2.540$ cm, t in μsec.

Rod No.	L cm	t_A	t_B	t_C	t_D	t_P	t_Q	t_R	t_S
14	2.54	4.21							
15	5.08	8.53	15.03				32.40	38.96	
16	10.16	17.19	23.75	30.30	37.04		52.38		
17	15.24	25.79	32.65	38.87	45.82		83.95		
18	20.32	34.44	41.25	47.24			110.38	117.10	
19	25.40	43.04	49.57	56.21	63.13		136.17	142.91	149.78

and V_R the velocity of rotational waves is given by

$$V_R=(\mu/\rho)^{\frac{1}{2}}. \tag{4}$$

Such a rotational wave must eventually strike the opposite side of the rod and there give rise to a reflected rotational wave and a dilatational wave at grazing reflection in order to satisfy the boundary conditions. This dilatational wave is the first delayed arrival corresponding to the time t_B.[5]

Referring to Fig. 4 and using the principles of geometrical optics, the above process corresponds to a path such as $\langle bqrd\rangle$, where $\langle bq\rangle$ and $\langle rd\rangle$ are traversed as dilatational waves, and $\langle qr\rangle$ is traversed as a rotational wave. There is an uncountably infinite set of such paths ($\langle astc\rangle$ and $\langle buvd\rangle$ are further examples) but all have the same travel time. The delay, Δt, incurred in taking the path $\langle bqrd\rangle$ instead of the path $\langle bc\rangle$ (traversed as a dilatational wave) is readily seen to be given by

$$\Delta t=(1/V_R)(D/\cos\theta)-(1/V_D)(D\sin\theta/\cos\theta), \tag{5}$$

where D is the diameter of the rod. Upon elimination of θ with Eq. (3) we find

$$\Delta t=D[(V_D^2-V_R^2)^{\frac{1}{2}}/V_D V_R]. \tag{6}$$

The above analysis is by no means limited to one such delay; the delayed dilatational wave may be carried through the same reasoning to yield a twice delayed dilatational wave corresponding to the path $\langle bqrstc\rangle$ in Fig. 4 and yet again to yield a dilatational wave delayed three times corresponding to the path $\langle bqrstuvd\rangle$ of Fig. 4, etc. Since the time for the undelayed dilatational wave to travel the length of the rod is L/V_D where L is the length of the rod, it is obvious that these arrival times are given by the relation

$$t=(L/V_D)+nD[(V_D^2-V_R^2)^{\frac{1}{2}}/V_D V_R], \quad n=0, 1, 2, \cdots, \tag{7}$$

where n is the number of times delayed.

This equation fits the arrivals at t_A, t_B, t_C, etc. quite accurately, but it requires a further extension to include the arrivals at t_P, t_Q, t_R, etc. This extension is readily obtained in terms of reflections from the ends of the rods.

[5] This transfer of mode process has been used in the making of delay lines. See *Supersonic Solid Delay Lines* NDRC Div. 14 OEMsr-262 Report No. 932 (April 30, 1946).

Referring to Table I, it is evident that the relations

$$t_P=3t_A,\quad t_Q=3t_A+\Delta t,\quad t_R=3t_A+2\Delta t,\quad t_S=3t_A+3\Delta t$$

are very closely satisfied. In other words t_P corresponds to a wave pulse which traversed the length of the rod three times as a dilatational wave, t_Q corresponds to a wave which traversed the rod in the same manner except delayed once, etc. Occasionally still higher types such as $5t_A+n\Delta t$, etc. are observed, but accurate reading of the arrival time is difficult.

From the above considerations it is apparent that all the arrival times considered can be represented by the equation

$$t=m(L/V_D)+nD[(V_D^2-V_R^2)^{\frac{1}{2}}/V_D V_R], \quad n=0, 1, 2, 3, \text{etc.}, \quad m=1, 3, 5, \text{etc.} \tag{8}$$

However, m and n are subject to the restriction

$$mL\geq nD\tan\theta, \tag{9}$$

since the wave must advance along the axis of the rod a distance $D\tan\theta$ during each delay, and the wave travels a total axial distance of mL.

The principles of geometrical optics employed here are generally valid when the wave-length is small compared to the smallest dimension involved. This condition is satisfied for the rods of Figs. 2 and 3, because the pulses involved consist of a frequency spectrum of roughly 1–5 megacycles, which corresponds to a dilatational wave-length of 0.12 cm to 0.6 cm in steel. However, a much more lucid justification for their use in the present instance is the simple fact that the transmitted pulses are so short that it is impossible for the first delayed wave train to interfere with the undelayed wave train, etc.

The situation when the successive wave trains interfere has also been investigated to some extent. Figure 5 is a photographic record obtained for the transmission of these same pulses through a series of samples of drill rod 15.240 cm in length and having diameters of 2.54, 1.27, 0.635, 0.3125, and 0.1565 cm, respectively.

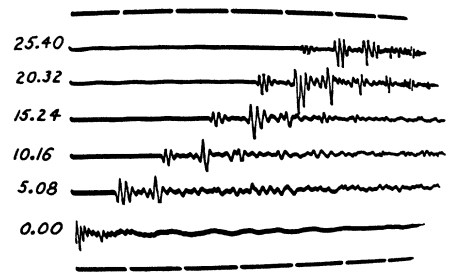

FIG. 3. Pulses through cold rolled steel rods 2.540 cm in diameter.

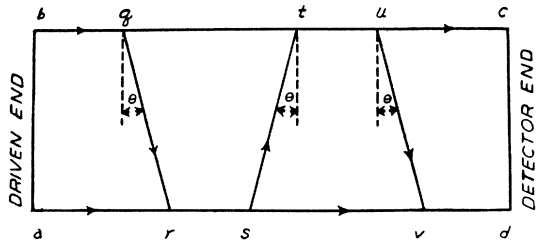

FIG. 4. Possible wave paths in rod.

The 2.54-cm and 1.27-cm rods give the characteristic patterns described above except that the undelayed wave is attenuated as the diameter decreases. This wave appears to be absent for the 0.635-cm rod but it can be seen on the oscilloscope screen. For the two smaller rods it could not be detected above the background. The characteristic decrease in delay with decrease in diameter is clearly shown, and, as this means production of more delayed wave trains for a rod of given length, the rapid decay of the primary (undelayed) wave pulse with decrease in diameter is certainly to be expected. However, the time of arrival of the undelayed wave does not change by any detectable amount. The traces for the 0.3125 cm and 0.1565 cm rods clearly indicate the interference possible between the various wave trains when the delay is shorter than the pulse duration.

These experimental results are in no way contrary to the theory of unending simple harmonic progressive waves on an infinite cylindrical bar as described by Pochhammer.[6] For such a wave interference would have its full effect. The infinite number of delayed wave trains would bring about complete destructive interference unless the delay, Δt, is exactly an integral number of vibrations. This is precisely the nature of the motions which are permitted in Pochhammer's solution. Using the methods employed by Cooper,[7] one should be able to pass from the steady state solutions of Pochhammer to the solution of the present transient problem.

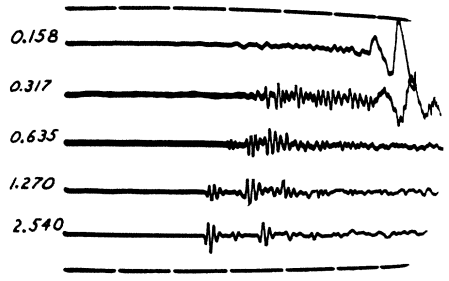

FIG. 5. Pulses through drill rods 15.240 cm in length.

[6] L. Pochhammer, J. F. Math. (Creele), Bd. 81 (1876), p. 324 also A. E. H. Love, Mathematical Theory of Elasticity, p. 287–291.
[7] J. L. B. Cooper, Phil. Mag. **38**, 1–22 (1947).

EXPERIMENTAL RESULTS

The principles of geometrical optics must be regarded as exact as far as the travel times of first arrivals are concerned. However, experimental error possibilities are fairly numerous in apparatus of the sort employed here. Consequently, a least squares solution was made in fitting the data of Table I and that of Table II to Eq. (8). For this purpose Eq. (8) was replaced by

$$t=\epsilon+m\beta L+n\alpha D, \tag{10}$$

where

$$\beta=1/V_D, \quad \alpha=(V_D^2-V_R^2)^{\frac{1}{2}}/V_D V_R,$$

and ϵ was a possible error in determining the time zero.

For the data of Tables I and II the following values of ϵ, α, and β were obtained (α and β are expressed in μsec./cm and ϵ in μsec.).

	ϵ	α	β
Table I	0.090	2.6176	1.7007
Table II	−0.063	2.6083	1.6971

These values together with the appropriate integers m and n will reproduce the data in the corresponding tables with a probable error of 0.05 μsec. when substituted into Eq. (10). This figure is satisfactorily close in view of the reading errors to be expected with the TS-100/AP oscilloscope.

From the definitions of α and β it is evident that V_D and V_R can be calculated from

$$V_D=1/\beta, \tag{11}$$

$$V_R=(\alpha^2+\beta^2)^{-\frac{1}{2}}. \tag{12}$$

The bulk modulus, K, and rigidity modulus, μ, can then be calculated from V_D, V_R and the density ρ by using Eqs. (2) and (4). The Young's modulus, E, and Poisson's ratio, σ, can then be found from the

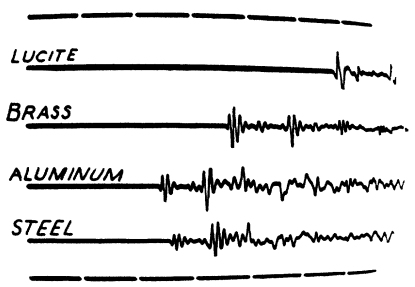

FIG. 6. Pulses through rods 2.540 cm in diameter, 15.240 cm in length.

equations

$$E=9\mu K/(3K+\mu), \tag{13}$$

$$\sigma=\frac{1}{2}\left(\frac{3K-2\mu}{3K+\mu}\right). \tag{14}$$

To date several materials other than the above samples of steel have been examined using a single rod 15.24 cm long and 2.540 cm in diameter. The totality of results is summarized in Table III. The velocities are given in meters/sec., and the elastic moduli in units of 10^{11} dynes/cm^2. The densities used are given in g/cm^3. Figure 6 is a photograph of the traces obtained with the additional materials with a cold rolled steel rod of the same length and cross section for comparison.

TABLE III. Summary of results.

Material	V_D	V_R	ρ	K	μ	E	σ
C. R. Steel I	5880.0	3203.5	7.82	16.34	8.025	20.69	0.289
C. R. Steel II	5892.2	3211.8	7.82	16.39	8.067	20.79	0.289
Aluminum	6379.0	3100.0	2.70	7.47	2.60	6.98	0.345
Brass	4283.0	2033.0	8.56	11.02	3.54	9.59	0.355
Lucite	2640.0	1269.0	1.18	5.70	1.90	5.13	0.350

PHYSICAL REVIEW VOLUME 75, NUMBER 10 MAY 15, 1949

Ferromagnetic Resonance at Microwave Frequencies in an Iron Single Crystal*

ARTHUR F. KIP AND ROBERT D. ARNOLD
Research Laboratory of Electronics, Massachusetts Institute of Technology, Cambridge, Massachusetts
(Received January 19, 1949)

Ferromagnetic resonance absorption in a single iron crystal has been observed at 23,675 and 9260 Mc/sec., using an external magnetic field applied perpendicular to the r-f magnetic field in the plane of the crystal surface. A variation in the resonance field is found which depends on the angle the magnetic field makes with the crystal axes. The results agree well with the theory of Kittel which predicts that an angular variation in resonance will result from the effects of crystal anisotropy. In the case of the lower frequency, deviations from the expected angular variation and a second resonance peak are shown to be the result of incomplete alignment of the magnetization with the direction of applied field. A calculation of the first-order anisotropy constant computed on the basis of this deviation agrees well with the known value.

INTRODUCTION

THE first experiment showing a microwave resonant absorption in iron was performed by Griffiths.[1] In this experiment a thin film of iron was applied to one end of a microwave resonant cavity. An external magnetic field was applied parallel to the surface of the thin film. With a constant microwave frequency, it was found that a maximum power absorption occurred for a particular value of external applied field.

Kittel[2] has discussed the theory of ferromagnetic resonance absorption and has shown that the resonance condition is given by

$$\omega_0=\gamma(BH)^{\frac{1}{2}}, \tag{1}$$

where ω_0 is the resonance frequency, $\gamma=ge/2mc$ = magnetomechanical ratio for electron spin, H is the static magnetic field, and B is the magnetic induction in the specimen. Kittel has further predicted that for single crystals the magnetic field for resonance should be dependent on the angle which the external field makes with the crystal axis, owing to the effect of anisotropy. In the present experiments the resonance phenomenon was investigated, using a single Fe–Si crystal, with the purpose of determining the effect of the known anisotropy of the crystal on resonance absorption.

THEORY

Before presenting the results of these experiments, a short discussion of the theory, as developed by Kittel, will be given. Ferromagnetic resonance absorption is to be expected, by analogy with the Purcell-Bloch nuclear resonance experiment, when the applied field is such that the microwave frequency is equal to the Larmor frequency for electron spin. It is shown that the demagnetization field normal to the surface of the crystal must be taken into account when calculating the Larmor frequency. The effect of crystalline anisotropy on resonance can be accounted for by treating the anisotropy energy in terms of an equivalent magnetic field. This treatment leads to the effective demagnetizing factor which is to be included in the calculation of the Larmor frequency, and results in a modification of Eq. (1).

In an infinite plane cubic crystal, the modified equation for resonance in the (100) plane is found

* This work has been supported in part by the Signal Corps, the Air Materiel Command and the ONR.
[1] J. H. E. Griffiths, Nature **158**, 670 (1946).
[2] C. Kittel, Phys. Rev. **73**, 155 (1948).